

Influence of the Switched Reluctance Machines design parameters on its steady-state operation characteristics

V. S. de C. Teixeira, D. N. Oliveira, R. S. T. Pontes, S. A. Viana
Universidade Federal do Ceará – Department of Electrical Engineering
Campus do Pici, P.O. Box: 6001,
Fortaleza – CE, ZIP Code: 60.455-760, Brazil

Abstract- This paper presents an analysis of the influence of the switched reluctance machine design parameters on its steady-state operation characteristics (phase inductance, phase current and mechanical output torque). The present analysis is carried out using computational simulation, based on the constructive parameters of a SRM designed by the authors. It is also suggested applications for incoming studies.

I. INTRODUCTION

The switched reluctance motor (SRM) is a very promising alternative for industrial applications mainly because it presents an easier assembly and maintenance.

In general, the SRM is best suited for industrial applications, which demand high efficient and fault tolerant machines [1]. However, some disadvantages of this machine, like vibration, acoustic noise and torque ripple, still prevent its use in widespread applications [2].

Many are the discussions regarding the SRM project techniques [3], which are mainly based upon the desired value for the output torque, similarly to the conventional machines design techniques. Since some parameters intervals provide a better performance of the machine, the project simulation provides a better knowledge about the parameters that have a greater influence on the machine output.

A computational simulation was implemented, using the MATLAB platform, in order to analyze the influence of the SRM design parameters on its steady-state operation characteristics.

II. SRM CONFIGURATION

According to [2] the industrial application of the SRM is limited due to some disadvantages like high ripple torque (intrinsic to the doubly-salient SRMs). Thus, the SRM design parameters have to be chosen in order to provide the best machine performance for the desired application.

The SRM prototype discussed in this paper (Fig. 1) has 6 stator poles and 4 rotor poles, and its parameters characteristics are shown in Table I.

III. ANALYTICAL METHOD FOR THE SRM SIMULATION

The analytical method used gives a good approximation of

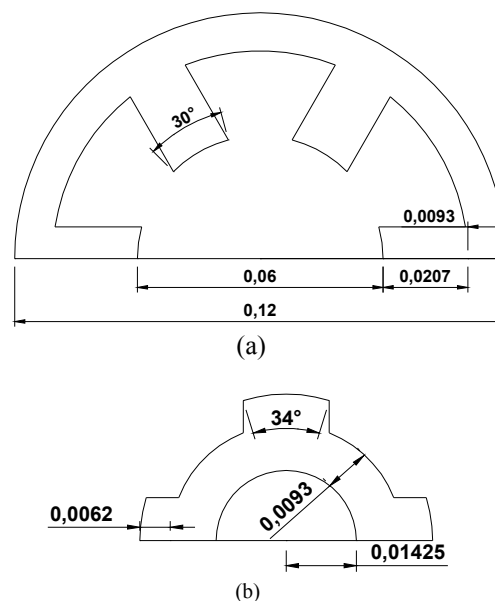


Fig. 1. SRM structure: (a) Stator dimensions (mm) and (b) rotor dimensions (mm)

TABLE I
SRM PARAMETERS

Parameter	Value	Parameter	Value
Power Output	736 W	Stator arc pole width	30°
Angular velocity	209 rad/s	Stack length	0.045 m
Turns per phase	110 V	Air gap length	0.00025 m
Nominal current	10 A	Rotor pole height	0.0062 m
Number of rotor poles	4	Stator pole height	0.0207 m
Number of stator poles	6	Rotor yoke thickness	0.0093 m
Rotor arc pole width	34°	Stator yoke thickness	0.0093 m
Bore diameter	0.060 m	External diameter	0.12 m
Phase winding resistance	0,2747 Ω	Wire type	17AWG

the SRM dynamic behavior. It is based on magnetization curves (flux, current) for a number of discrete rotor position angles and current, developed by R. Krishnan [3].

For each one of these position, the magnetic flux, which passes through the magnetic core and the air gap, is subdivided in different paths with a specific length, cross sectional area and permeance values. Thus, the computational simulation of the analytical method evaluates the SRM electrical performance on its steady-state operation.

A. Considerations for the analytical method – Flux Lines

The following assumptions are made to compute the response of the machine [3]:

- flux distribution is uniform over the cross section of the core;
- the flux lines enter and leave the iron surface like normal vectors;
- the air gap sections of the flux lines consist of straight lines and concentric arc segments;
- the flux lines in the stator and translator poles run parallel to each pole axis;
- the flux lines in the stator and translator yokes run parallel to the longitudinal axis;
- the magnetic core of the machine has a known magnetization curve.

B. Consideration for the analytical method – Current

According to [3-4] a good quality approximation for the phase current profile is shown in Fig. 2.

According to Fig. 1, and considering a one-pole pair phase SRM, with current control, it is verified an increase in the phase current (right after it is turned on), until it reaches a reference value (i_{ref}), which, during the nominal steady-state operation of the machine, is equal to i_{nom} . The magnitude of the current oscillations, over the nominal current value, depend on the current control strategy chosen for the SRM drive system.

When the phase current is turned off, it starts decreasing rapidly, until the moment that the flux linkage is reversed, due to the phase inductance, slowing down the current fall time,

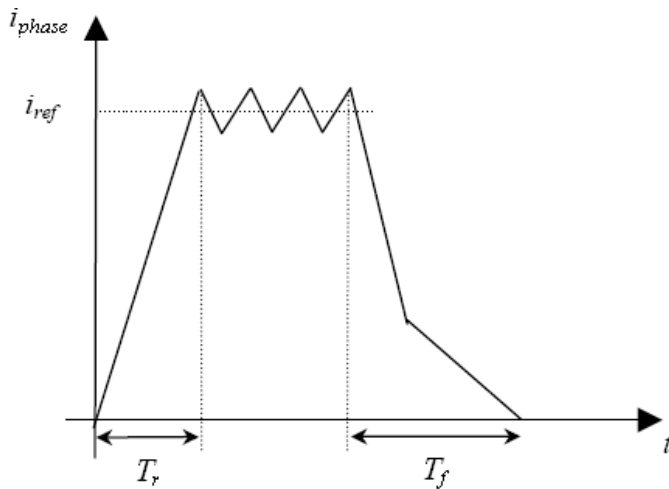


Fig. 2. General current profile, with hysteresis control, for one SRM phase.

until it reaches zero. After that, this current cycle restarts for the next SRM phase.

The current rise and fall time intervals are obtained using (1) and (2), respectively [2]:

$$T_r = \frac{(\Delta \theta_r)}{\omega_m} = \tau_u \cdot \ln \left(\frac{1}{1 - \frac{R_s \cdot i_{ref}}{V_{phase}}} \right) \quad (1)$$

$$T_f = \frac{(\Delta \theta_f)}{\omega_m} = \tau_a \cdot \ln \left(1 + \frac{R_s \cdot i_{ref}}{V_{phase}} \right) \quad (2)$$

where:

V_{phase}	→	phase voltage
ω_m	→	angular speed
$\Delta \theta_r$	→	current rise angular interval
$\Delta \theta_f$	→	current fall angular interval
T_r	→	current rise time interval
T_f	→	current fall time interval
τ_u	→	time constant of the unaligned inductance
τ_a	→	time constant of the aligned inductance
R_s	→	phase winding resistance

The values of τ_u and τ_a are obtained using (3) and (4) respectively:

$$\tau_u = \frac{L_{min}}{R_s} \quad (3)$$

$$\tau_a = \frac{L_{max}}{R_s} \quad (4)$$

The simulation was carried out only for one phase of the machine. The other phases were estimated based on the simulated phase, through adequate phase angular displacement and piecewise cubic Hermite interpolating polynomial.

IV. RESULTS AND DISCUSSIONS

The results for the nominal design values (Table I) of the machine parameters are shown in Table II and Fig. 3, 4, 5 and 6.

Simulations (implemented on the MATLAB® platform) were carried out considering variations of -10%, -5%, 5% and 10%, relative to the nominal values of the machine. The behavior of each output parameter, based on simulations

using the proposed analytical method, is shown in the following subsections.

The instantaneous torque and copper losses were calculated using (5) and (6), respectively [3]:

$$T = \frac{i^2}{2} \cdot \frac{(dL)}{(d\theta)} \quad (5)$$

$$P_c = R_s \cdot i^2 \quad (6)$$

where:

- T → instantaneous torque
- i → instantaneous current
- dL → incremental inductance
- $\Delta\theta$ → incremental angular displacement
- P_c → instantaneous copper losses

A. Average Torque

The simulation results for the average torque value are shown in Table III.

The design parameters which had greater influence on the average torque were the number of turns per phase and rotor arc pole width. It is also verified that the stator yoke does not influence the output average torque value.

B. Torque ripple

The simulation results for the torque ripple are shown in Table IV.

TABLE II
NOMINAL VALUES

Parameter	Average torque (N*m)	Torque ripple (N*m)	Copper losses (W)	Machine average weight (kg)
Value	1,2068	0,8542	30,7361	2,2639

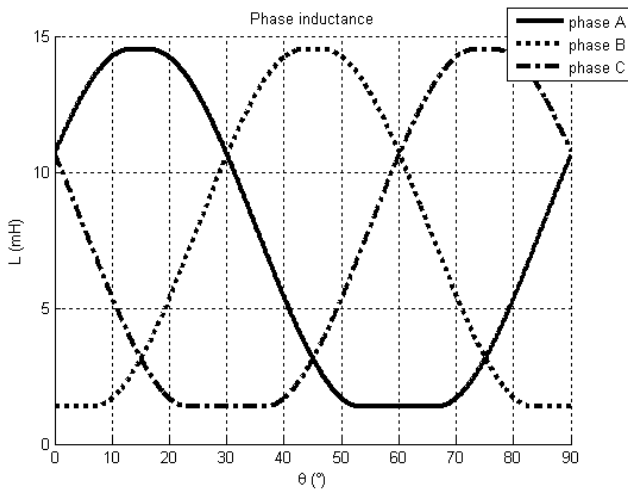


Fig. 3. Phase inductance simulation results for the nominal SRM.

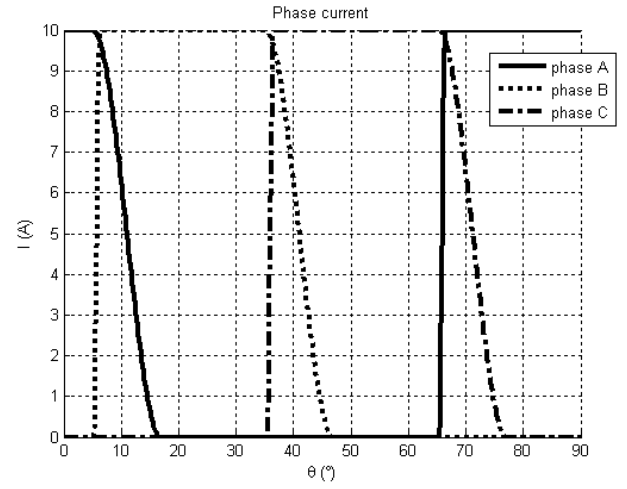


Fig. 4. Phase current simulation results for the nominal SRM parameters.

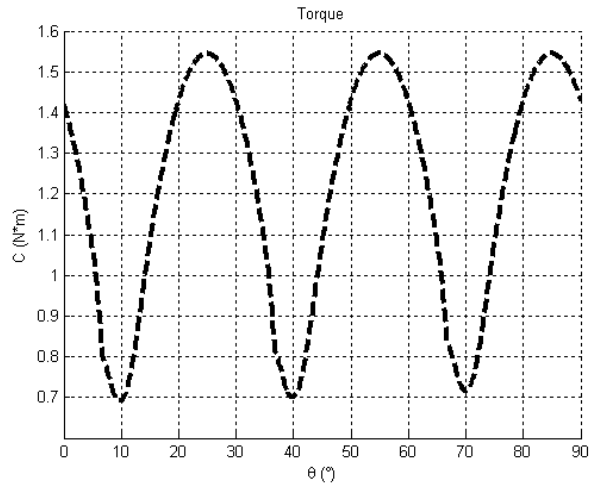


Fig. 5. Total torque simulation result for the nominal SRM parameters.

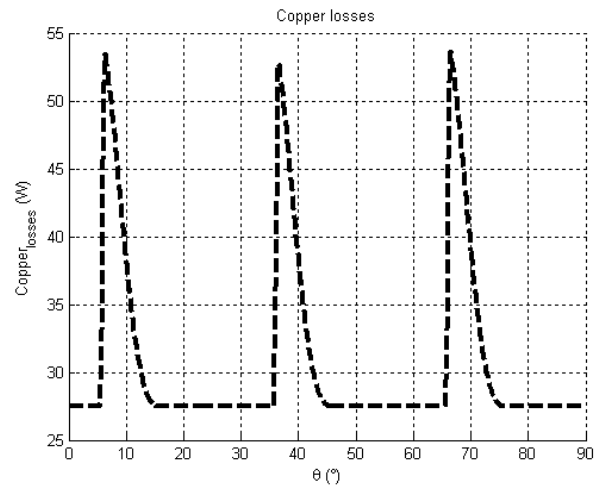


Fig. 6. Total copper losses simulation result for the nominal SRM.

It is verified that the design parameters influence for the torque ripple are very similar to the that of the average torque.

C. Copper losses

The simulation results for the copper losses are shown in Table V.

In this case, the design parameters which had greater influence on the copper losses were the number of turns per phase, the stack length and the stator arc pole width. The influence of this last parameter for the copper losses is straightforward, since the phase windings are concentrated on the stator poles.

D. Machine average weight

The simulation results for the machine average weight are shown in Table VI. For the calculation of this output parameter, the machine chassis weight was neglected. The weight of the wire (17AWG) and the density of both machine and shaft iron were considered to be $9,7067 \times 10^{-3} \text{ kg/m}$ and 7.700 kg/m^3 , respectively [6].

For this last case, the parameters which accounted for the machine average weight were the stack length and the yoke thickness of both rotor and stator.

V. CONCLUSION

The proposed analytical method provided a quantitative

TABLE III
AVERAGE TORQUE

Parameter	Percentual variation (%)			
	-10%	-5%	5%	10%
Turns per phase	-10,76	-4,79	5,81	10,67
Rotor arc pole width	-4,34	-2,37	1,15	1,41
Stator arc pole width	-8,90	-4,43	2,73	4,55
Stack length	-10,33	-5,36	5,25	10,39
Air gap length	0,02	-0,04	-0,07	-0,02
Rotor pole height	-2,06	-1,02	0,95	1,90
Stator pole height	0,92	0,46	-0,45	-1,06
Rotor yoke thickness	-3,01	-1,31	0,49	0,49
Stator yoke thickness	-3,01	-1,31	0,49	0,49

TABLE IV
TORQUE RIPPLE

Parameter	Percentual variation (%)			
	-10%	-5%	5%	10%
Turns per phase	-5,42	-2,36	2,82	5,15
Rotor arc pole width	28,39	18,27	-11,46	-16,57
Stator arc pole width	65,49	35,37	-20,7	-40,26
Stack length	-5,6	-2,88	2,76	5,47
Air gap length	0,01	-0,04	-0,05	-0,01
Rotor pole height	-1,18	-0,62	0,55	1,05
Stator pole height	0,62	0,27	-0,34	-0,73
Rotor yoke thickness	-1,74	-0,75	0,27	0,27
Stator yoke thickness	-1,74	-0,75	0,27	0,27

TABLE V
COPPER LOSSES

Parameter	Percentual variation (%)			
	-10%	-5%	5%	10%
Turns per phase	-1,03	-0,45	0,54	0,98
Rotor arc pole width	-0,1	-0,03	-0,01	-0,05
Stator arc pole width	-1,07	-0,51	0,41	0,7
Stack length	-1,07	-0,55	0,54	1,06
Air gap length	0	-0,01	-0,01	0
Rotor pole height	-0,23	-0,12	0,11	0,21
Stator pole height	0,12	0,05	-0,07	-0,14
Rotor yoke thickness	-0,34	-0,14	0,05	0,05
Stator yoke thickness	-0,34	-0,14	0,05	0,05

TABLE VI
MACHINE AVERAGE WEIGHT

Parameter	Percentual variation (%)			
	-10%	-5%	5%	10%
Turns per phase	-1,72	-0,78	0,94	1,72
Rotor arc pole width	-0,17	-0,08	0,08	0,17
Stator arc pole width	-0,94	-0,47	0,47	0,94
Stack length	-9,55	-4,89	4,89	9,55
Air gap length	-0,03	-0,01	0,02	0,03
Rotor pole height	-0,92	-0,46	0,46	0,92
Stator pole height	-2,38	-1,14	1,14	2,39
Rotor yoke thickness	-5,15	-2,87	2,9	5,23
Stator yoke thickness	-5,15	-2,87	2,9	5,23

and qualitative understanding of the influence of the SRM design parameters on the machine output characteristics.

Based on the simulations, the designer can adequately balance the desired output characteristics of the SRM, in order to obtain a suitable project for the specific application.

ACKNOWLEDGMENT

The authors gratefully acknowledge the Agency for Scientific and Technological Development of the state of Ceará (FUNCAP) for the financial support.

REFERENCES

- [1] Arthur V. Radun. "Design Considerations for the Switched Reluctance Motor", IEEE Transactions on Industry Applications, vol. 31, no.5, pp. 1079-1087, September/October 1995.
- [2] Yasuharu Ohdachi, "Optimum designer of switched reluctance motors using dynamic finite element analysis", IEEE Transactions on Magnetics, vol. 33, no.2, pp. 2033-2036, March, 1997.
- [3] R. Krishnan, Switched Reluctance Motor Drives –

Modeling, Simulation, Analysis, Design and Applications. New York, CRC Press, 2001.

- [4] Materu, P. N. and R. Krishnan. "Steady-State Analysis of the Variable-Speed Switched-Reluctance Motor Drive", IEEE Transactions on Industrial Electronics, vol. 36, no.4, pp. 523-529, November 1989.
- [5] P.J. Lawrenson, et al. "Variable-speed Switched Reluctance Motors", IEE proc., part. B, vol. 127, no. 4, pp. 253-265, July 1980.
- [6] Acesita, Inc. "Electrical steel catalogue – Grain Oriented and Grain Non-Oriented Silicium", found at <http://www.acesita.com.br>, July 2007.